A Modified Discontinuous Modulation Signal Based on 12-Sector SVPWM with Modulation Offset Injection for a Vienna Rectifier

Ong-ard Tubburee
Department of Industrial Electrical Technology, Faculty of Industrial Technology, Valaya Alongkorn Rajabhat University under the Royal Patronage, Pathum Thani, Thailand
ongart.tub@vru.ac.th

Sitthisak Audomsi
Faculty of Engineering, Mahasarakham University, Maha Sarakham, Thailand
Sitthisak.seagame@gmail.com

Worawat Sa-ngiamvibool
Faculty of Engineering, Mahasarakham University, Maha Sarakham, Thailand | Electrical and Computer Engineering Research Unit, Mahasarakham University, Maha Sarakham, Thailand
wor.nui@gmail.com

Kanyarat Ek-iam
Department of Industrial Electrical Technology, Faculty of Industrial Technology, Valaya Alongkorn Rajabhat University under the Royal Patronage, Pathum Thani, Thailand
kanyarat@vru.ac.th (corresponding author)

Received: 10 October 2025 | Revised: 22 November 2025 | Accepted: 9 December 2025

 DOI: https://doi.org/10.48084/etasr.15439

ABSTRACT

The increasing demand for high-efficiency AC–DC conversion in modern power systems, such as Electric Vehicle (EV) charging, renewable energy integration, and industrial motor drives, has intensified research into advanced modulation techniques for Vienna rectifier. Conventional 6-sector Space Vector Pulse Width Modulation (SVPWM) strategies often suffer from limited modulation flexibility and insufficient performance at low modulation indices, where high DC-link voltage operation is required. To address these challenges, this paper proposes a modified discontinuous modulation signal based on a novel 12-sector SVPWM combined with a topology-aware switching scheme and modulation offset injection. A seven-segment switching sequence is designed for the proposed 12 sectors, enabling effective generation of Discontinuous PWM (DPWM) waveforms, improved current shaping, and Power Factor Correction (PFC). The simulation results indicate that the proposed method achieves a 9.24% reduction in Total Harmonic Distortion (THD) in the low-modulation region (m_a<0.50) compared to the conventional method. Furthermore, dynamic tests confirm robust transient response under DC-link voltage steps, stable capacitor voltage balancing, and minimized switching commutation. These results demonstrate that the proposed modulation approach significantly enhances power quality, efficiency, and dynamic performance, making it a promising solution for next-generation high-performance Vienna rectifier systems.

Keywords-Vienna rectifier; SVPWM; discontinuous PWM; 12-sector; modulation offset

I. INTRODUCTION

Pulse Width Modulation (PWM) rectifiers have garnered significant attention across a wide range of applications, including EV chargers, wind energy systems, telecommunication power supplies, welding equipment, and Uninterruptible Power Systems (UPS) [1-3]. Their widespread use is primarily driven by their capability to ensure high input Power Quality (PQ), maintain near-unity Power Factor (PF), and precisely regulate the DC-link voltage via controlled semiconductor switching [4]. Among various PWM rectifier topologies, the Vienna rectifier, as illustrated in Figure 1,

stands out as an effective solution for unidirectional AC–DC conversion. Its three-level structure, reduced number of Controllable Power Switches (CPSs), and the ability to limit device voltage stress to half of the DC-link voltage collectively enable high efficiency, compact design, and robust performance [5-6]. To enhance the modulation performance of the Vienna rectifier, several techniques have been explored, including Carrier-Based PWM (CB-PWM), Space Vector Modulation (SVM), and SVPWM. While CB-PWM is simple to implement, it suffers from increased midpoint voltage ripple and poor DC-link voltage utilization [7, 8]. Conversely, SVM offers improved current quality and better midpoint voltage control, though at the expense of increased computational complexity due to sector identification and coordinate transformation [9, 10]. To overcome this trade-off, simplified SVPWM methods have been introduced, combining the benefits of CB-PWM and SVM by directly generating switching signals based on preselected voltage vectors and triangular carrier comparison [11, 12]. The switching sequence plays a critical role in these methods. In particular, the five-segment sequence, which leads to DPWM, reduces switching losses by eliminating redundant commutations, making it suitable for high-efficiency applications [13]. However, it may restrict voltage vector synthesis in certain regions. Alternatively, the seven-segment sequence, although more common in other multilevel converters, can improve input current quality, thermal distribution, and voltage balance. Despite its benefits, its use in Vienna rectifiers remains underexplored.

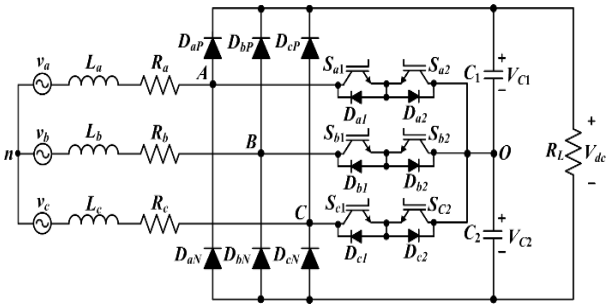

Fig. 1. Topological structure of the Vienna rectifier.

This work proposes a novel 12-sector SVPWM strategy that incorporates a seven-segment switching sequence and a modulation offset injection algorithm for the Vienna rectifier. The method enhances vector resolution and introduces controlled zero-voltage intervals to reduce switching commutations. The resulting discontinuous modulation waveforms are compared with a triangular carrier to generate efficient switching signals within the linear modulation index region, thereby preventing distortion of high-amplitude input currents. Operating in the linear region also enables the proposed rectifier to achieve higher output-voltage boosting capability as the modulation index decreases. This approach aligns with the rectifier's operational constraints while improving PQ and reducing losses. Comprehensive simulation studies validate the effectiveness of the proposed method compared to the conventional 6-sector SVPWM.

II. OPERATING ANALYSIS OF THE VIENNA RECTIFIER

The operation of the Vienna rectifier is primarily determined by the direction of the input current and the switching states of the CPSs in each bridge arm. During the positive half-cycle, when both CPSs are turned ON, the current flows through the path $v_k \rightarrow L_k \rightarrow R_k \rightarrow S_{k1} \rightarrow D_{k2}$, as shown in Figure 2(a), where the subscript k denotes the corresponding phase (i.e., a, b, c). When both CPSs are OFF, the current bypasses the bidirectional switch and flows through $v_k \rightarrow L_k \rightarrow R_k \rightarrow D_{kp} \rightarrow C_1$, as depicted in Figure 2(b). Conversely, during the negative half-cycle, if both CPSs are ON, the conduction path reverses to $S_{k2} \rightarrow D_{k1} \rightarrow R_k \rightarrow L_k \rightarrow v_k$, as portrayed in Figure 2(c). When both CPSs are OF, current flows through $C_2 \rightarrow D_{kn} \rightarrow R_k \rightarrow L_k \rightarrow v_k$, as illustrated in Figure 2(d). This current path analysis confirms the absence of short-circuit conditions between bridge arms. It demonstrates the rectifier's ability to generate three distinct output voltage levels: $+V_{dc}/2$, 0, and $-V_{dc}/2$, each limited to half the DC-link voltage. Moreover, the voltages across the two output capacitors naturally alternate throughout the switching cycle. Therefore, when the CPSs are properly controlled to satisfy these operating conditions, inherent voltage balancing between the capacitors can be achieved without the need for additional control circuitry.

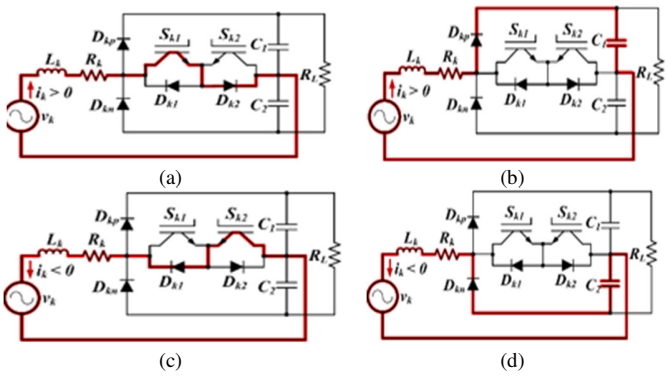

Fig. 2. Current direction analysis of Vienna rectifier: (a)–(b) positive input current with CPSs ON and OFF, respectively; (c)–(d) negative input current with CPSs ON and OFF, respectively.

III. 12-SECTOR DISCONTINUOUS SVPWM BASED ON THREE-PHASE CURRENT DIRECTION

According to rectification principles, the main objective of a rectifier is to deliver the phase current with the highest instantaneous value to the load. To achieve this, the switching states of the CPSs in each phase must be configured to ensure that the phase carrying the maximum input current continuously conducts through the appropriate path, thereby maintaining a unity PF. In the proposed Vienna rectifier, this goal requires dynamic adaptation of the CPS switching states to real-time current conditions to optimize conduction and power transfer. However, when the SVM technique is applied to generate modulation waveforms, the original switching states of certain voltage vectors may differ from those in the conventional space vector diagram. This matter is illustrated in Figure 3, which compares the original switching states with

those determined by the space vector diagram. Such mismatches can result in suboptimal current shaping or unintended power flow, which must be carefully addressed during modulation design. To resolve this issue, the proposed approach introduces a topology-aware correction mechanism that aligns SVM-generated modulation waveforms with the Vienna rectifier's inherent operating principles. This ensures proper current shaping, optimized power flow, effective capacitor voltage balancing, and improved overall performance.

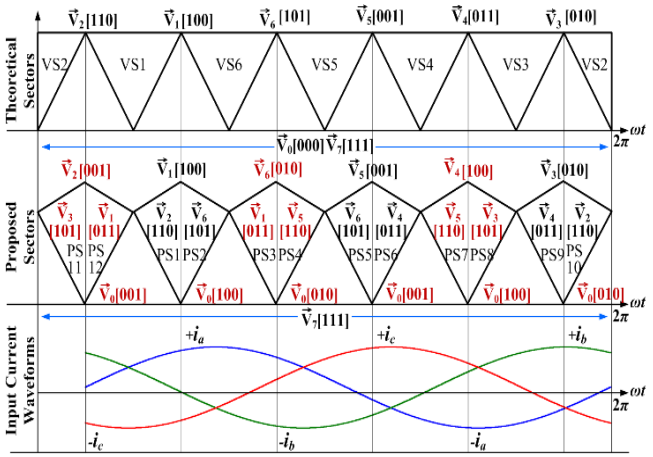

Fig. 3. Relationship between the proposed 12-sector and three-phase current direction based on the conventional 6-sector SVM.

The proposed 12-sector space vector division, denoted as PS_i (i=1,2,...,12), is determined based on the real-time sign of the three-phase line currents. This finer segmentation enables more precise control of the current path in accordance with the instantaneous current direction. In contrast, the conventional SVM employs only 6 theoretical voltage sectors, VS_j (j = 1,2, ...6), assuming balanced and symmetrical three-phase voltages such that $v_a+v_b+v_c=0$. These voltages are transformed into a two-axis stationary αβ reference frame using the Clarke Transformation:

$$\begin{bmatrix} v_\alpha \\ v_\beta \end{bmatrix} = \begin{bmatrix} 1 & -\frac{1}{2} & -\frac{1}{2} \\ 0 & \frac{\sqrt{3}}{2} & -\frac{\sqrt{3}}{2} \end{bmatrix} \begin{bmatrix} v_a \\ v_b \\ v_c \end{bmatrix} \quad (1)$$

The average value of the reference voltage vector (V_{ref}), which rotates continuously within the space vector diagram, can be determined using the general expression of space vector synthesis. This value is represented in the αβ frame and is given by:

$$\vec{V}_{ref} = v_\alpha + jv_\beta = \frac{2}{3}\left[v_a e^{j0} + v_b e^{j\frac{2\pi}{3}} + v_c e^{j\frac{4\pi}{3}}\right] \quad (2)$$

For example, when V_{ref} lies within sector VS_1, it is synthesized using the adjacent non-null vectors V_1, V_2, and null vectors V_0, V_7, ensuring volt-second balance across the switching period (T_s). The SVM principle is then articulated as:

$$\vec{V}_{ref}T_S = \frac{2}{3}V_{dc}\left[t_1 + t_2 + \frac{T_0}{2} + \left(t_2 + \frac{T_0}{2}\right)\left(-\frac{1}{2} + j\frac{\sqrt{3}}{2}\right) + \frac{T_0}{2}\left(-\frac{1}{2} - j\frac{\sqrt{3}}{2}\right)\right] \quad (3)$$

where t_1 and t_2 are the dwell times for the non-null vectors V_1 and V_2, respectively, and T_0 is the combined duration of the two null vectors (t_0+t_7). To solve for the dwell times t_1 and t_2, (3) is separated into its α and β components:

$$t_1 = \frac{\sqrt{3}}{V_{dc}}\left[\frac{\sqrt{3}}{2}v_\alpha T_S - \frac{1}{2}v_\beta T_S\right], t_2 = \frac{\sqrt{3}}{V_{dc}}\left[v_\beta T_S\right], T_0 = T_S - t_1 - t_2 \quad (4)$$

In conventional modulation designs for the Vienna rectifiers, a five-segment switching sequence technique using two non-null vectors and only one null vector (e.g., V_7=[111]) is commonly applied to achieve DPWM. However, this study proposes an improved seven-segment switching sequence strategy aligned with the newly defined 12-sector SVPWM. For instance, when V_{ref} falls within VS_1, it overlaps proposed sectors PS_1 and PS_{12}. Within PS_1, a symmetric seven-segment sequence $V_7V_2V_1V_0V_1$ V_2V_7 is employed, corresponding to the switching logic sequence [111]-[110]-[100]-[000]-[100]-[110]-[111]. Each binary vector represents the switching states of the bidirectional switches S_a, S_b, and S_c. Based on this pattern, the conduction intervals for each bridge leg (T_a, T_b, and T_c) are described in:

$$T_a = t_1 + t_2 + T_0/2, T_b = t_2 + T_0/2, T_c = T_0/2 \quad (5)$$

The new modulation waveform equations in the αβ frame are generated from these time intervals as:

$$\begin{cases} v_{ma} = \frac{1}{2} - \frac{\sqrt{3}}{4V_{dc}}\left[-\sqrt{3}v_\alpha - v_\beta\right] \\ v_{mb} = \frac{1}{2} - \frac{\sqrt{3}}{4V_{dc}}\left[\sqrt{3}v_\alpha - 3v_\beta\right] \\ v_{mc} = \frac{1}{2} - \frac{\sqrt{3}}{4V_{dc}}\left[\sqrt{3}v_\alpha + v_\beta\right] \end{cases} \quad (6)$$

Using this approach, modulation signal expressions for all proposed 12 sectors can be systematically developed. The resulting modulation waveforms for a-phase (vma) over a full switching cycle are shown in Figure 4(a).

IV. DISCONTINUOUS PWM GENERATION USING MODULATION OFFSET INJECTION

A. Analysis of Modulation Signals

In conventional 7-segment switching schemes, the space vector diagram is rearranged to produce continuous switching patterns, ensuring balanced three-phase voltage synthesis for three-phase inverters. This typically results in symmetrical modulation signals centered around a reference axis, with amplitude proportional to the modulation index, as illustrated in Figure 4(a). However, directly applying these signals in the Vienna rectifier does not yield the desired DPWM behavior due to its unidirectional current flow and bidirectional switch architecture. To enable discontinuous operation, the switching states must be adjusted based on the current direction and topological constraints of the proposed rectifier. This adjustment modifies the modulation signals such that, during peak input current intervals, discontinuities appear while

maintaining symmetry elsewhere. Figure 4(b) presents these characteristics. However, outside these intervals, the modulation signals still exhibit symmetrical behavior similar to the conventional continuous PWM. This behavior contrasts with the ideal modulation signals for PWM-controlled rectifiers operating in the Discontinuous Conduction Mode (DCM), where the modulation signal is expected to be clamped to the reference axis and vary its amplitude only toward the maximum value of 1. In some cases, the signal may be clamped at logic "1" and decrease toward the reference axis, depending on input current direction and switching constraints [14, 15].

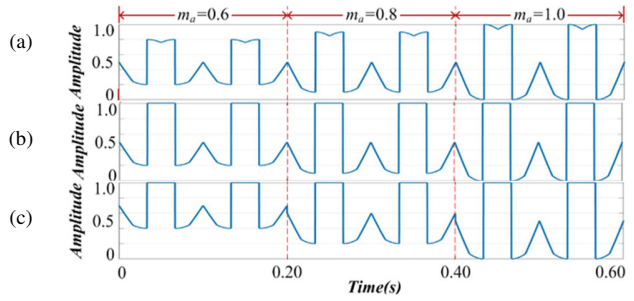

Fig. 4. A-phase modulation signals for m_a=0.6, 0.8, and 1.0: (a) conventional SVPWM, (b) modified discontinuous SVPWM, and (c) proposed discontinuous SVPWM with offset injection.

B. Modulation Offset Injection

Based on the working analysis of the Vienna rectifier, it is essential that the CPS in each bridge arm remain continuously turned ON during the time when the corresponding phase input current reaches its peak. To meet this requirement, the modulation waveforms previously displayed in Figure 4(b) are refined by superimposing a modulation offset signal (v_{mf}), defined as:

$$v_{mf} = \frac{1-m_a}{2} \quad (7)$$

where ma is the SVM modulation index (0<ma≤1.0), calculated from the Vref and DC-link voltage as:

$$m_a = \frac{\sqrt{3}V_{ref}}{V_{dc}} \quad (8)$$

This offset is uniformly applied across all proposed 12 sectors to maintain proper switching alignment with the conduction requirements of the Vienna rectifier. The resulting updated modulation signals incorporate both the sector-based switching logic and the injected offset, enabling accurate DPWM generation. An example of the offset-modified waveform for the a-phase CPS is shown in Figure 4(c). Finally, the gate signals are derived by comparing these updated modulation waveforms with a 12 kHz triangular carrier using a standard PWM comparator. A summary of the resulting new modulation signal equations for all phases across the 12 sectors is presented in Table I.

TABLE I. THREE-PHASE MODULATION SIGNAL EQUATIONS FOR THE PROPOSED 12-SECTOR

PSs	New modulation waveform equations
1	$v'_{ma}=1, v'_{mb}=1+\frac{m_a}{2}-\frac{\sqrt{3}}{4V_{dc}}[\sqrt{3}v_\alpha-3v_\beta]$, $v'_{mc}=1+\frac{m_a}{2}-\frac{\sqrt{3}}{4V_{dc}}[\sqrt{3}v_\alpha+v_\beta]$
2	$v'_{ma}=1+\frac{m_a}{2}-\frac{\sqrt{3}}{4V_{dc}}[\sqrt{3}v_\alpha+v_\beta]$, $v'_{mb}=1+\frac{m_a}{2}-\frac{\sqrt{3}}{4V_{dc}}[-\sqrt{3}v_\alpha+3v_\beta], v'_{mc}=1$
3	$v'_{ma}=1+\frac{m_a}{2}-\frac{\sqrt{3}}{2V_{dc}}[\sqrt{3}v_\alpha]$, $v'_{mb}=1+\frac{m_a}{2}-\frac{\sqrt{3}}{2V_{dc}}[v_\beta], v'_{mc}=1$
4	$v'_{ma}=1+\frac{m_a}{2}-\frac{\sqrt{3}}{2V_{dc}}[-\sqrt{3}v_\alpha], v'_{mb}=1,$ $v'_{mc}=1+\frac{m_a}{2}-\frac{\sqrt{3}}{2V_{dc}}[v_\beta]$
5	$v'_{ma}=1+\frac{m_a}{2}-\frac{\sqrt{3}}{4V_{dc}}[-\sqrt{3}v_\alpha+v_\beta], v'_{mb}=1,$ $v'_{mc}=1+\frac{m_a}{2}-\frac{\sqrt{3}}{4V_{dc}}[\sqrt{3}v_\alpha+3v_\beta]$
6	$v'_{ma}=1, v'_{mb}=1+\frac{m_a}{2}-\frac{\sqrt{3}}{4V_{dc}}[-\sqrt{3}v_\alpha+v_\beta]$, $v'_{mc}=1+\frac{m_a}{2}-\frac{\sqrt{3}}{4V_{dc}}[-\sqrt{3}v_\alpha-3v_\beta]$
7	$v'_{ma}=1, v'_{mb}=1+\frac{m_a}{2}-\frac{\sqrt{3}}{4V_{dc}}[-\sqrt{3}v_\alpha+3v_\beta]$, $v'_{mc}=1+\frac{m_a}{2}-\frac{\sqrt{3}}{4V_{dc}}[-\sqrt{3}v_\alpha+v_\beta]$
8	$v'_{ma}=1+\frac{m_a}{2}-\frac{\sqrt{3}}{4V_{dc}}[-\sqrt{3}v_\alpha-3v_\beta]$, $v'_{mb}=1+\frac{m_a}{2}-\frac{\sqrt{3}}{4V_{dc}}[\sqrt{3}v_\alpha-3v_\beta], v'_{mc}=1$
9	$v'_{ma}=1+\frac{m_a}{2}-\frac{\sqrt{3}}{2V_{dc}}[-\sqrt{3}v_\alpha]$, $v'_{mb}=1+\frac{m_a}{2}-\frac{\sqrt{3}}{2V_{dc}}[-v_\beta], v'_{mc}=1$
10	$v'_{ma}=1+\frac{m_a}{2}-\frac{\sqrt{3}}{2V_{dc}}[\sqrt{3}v_\alpha], v'_{mb}=1,$ $v'_{mc}=1+\frac{m_a}{2}-\frac{\sqrt{3}}{2V_{dc}}[-v_\beta]$
11	$v'_{ma}=1+\frac{m_a}{2}-\frac{\sqrt{3}}{4V_{dc}}[\sqrt{3}v_\alpha-v_\beta]$, $v'_{mb}=1, v'_{mc}=1+\frac{m_a}{2}-\frac{\sqrt{3}}{4V_{dc}}[-\sqrt{3}v_\alpha-3v_\beta]$
12	$v'_{ma}=1, v'_{mb}=1+\frac{m_a}{2}-\frac{\sqrt{3}}{4V_{dc}}[\sqrt{3}v_\alpha-v_\beta]$, $v'_{mc}=1+\frac{m_a}{2}-\frac{\sqrt{3}}{4V_{dc}}[\sqrt{3}v_\alpha+3v_\beta]$

V. RESULTS AND DISCUSSION

To verify the feasibility and performance of the proposed 12-sector SVPWM modulation strategy with modulation offset injection for the Vienna rectifier, a simulation model was built using MATLAB/Simulink. The key parameters of the power stage utilized in the simulation are summarized in Table II. In addition, a conventional vector-based current control method is

employed to ensure accurate input current shaping and regulate the DC-link voltage under varying operating conditions [16].

Figure 5 compares the current THD input of the conventional 6-sector SVPWM and the proposed 12-sector SVPWM, both operated without a PFC controller. The proposed method consistently achieves lower THD across most of the modulation index (ma) range. In the low-modulation region (ma<0.50), a notable improvement is observed: the average THD decreases from 29.47% (conventional) to 26.74% (proposed), corresponding to a 9.24% relative reduction. At higher modulation indices (ma>0.5), the gap narrows; however, the proposed technique continues to yield superior performance, maintaining THD levels between 23% and 24%, compared to 25%–26% for the conventional approach. These results highlight the suitability of the proposed method for Vienna rectifiers operating as unidirectional boost-type converters, where low-modulation index operation is common due to high DC-link voltage requirements.

TABLE II. MAIN CIRCUIT PARAMETERS USED IN THE SIMULATION

Parameters	Symbols	Value
AC input voltage (RMS)	V_a,V_b,V_c	110 V
Fundamental frequency	f_1	50 Hz
Input inductance	L_k	5 mH
Input resistance	R_k	5 Ω
Rated power	P_{reted}	5 kW
DC-link capacitance	C_1 and C_2	2200 μF

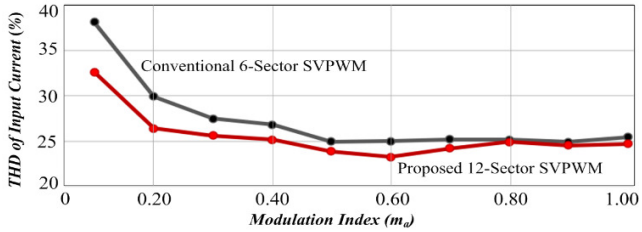

Fig. 5. Input current THD comparison between the proposed 12-sector and conventional 6-sector SVPWM methods without PFC control.

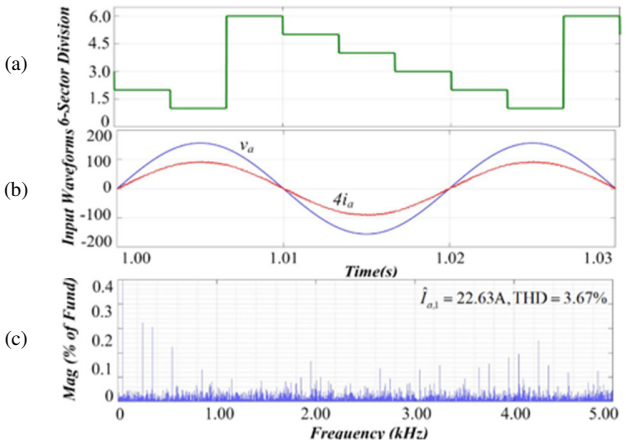

Fig. 6. Steady state results of the proposed rectifier operating under the conventional 6-sector SVPWM with PFC controller: (a) the 6-sector signal, (b) a-phase voltage and current waveforms, (c) a-phase current THD.

Figures 6 and 7 illustrate the steady-state input current quality of the Vienna rectifier operating with a PFC controller under two modulation strategies. In Figure 6(a), the conventional 6-sector SVPWM is applied. The magnified view of the a-phase input current and its corresponding phase voltage in Figure 6(b) shows that the current waveform is nearly sinusoidal and in phase with the voltage. The measured peak amplitude of the input current is 22.63 A, with a THD of 3.67%, as presented in Figure 6(c). In contrast, Figure 7 displays the proposed 12-sector SVPWM. The waveforms in Figure 7(b) reveal improved current smoothness, reduced distortion, and maintained phase alignment with the corresponding phase voltage. Furthermore, the harmonic spectrum in Figure 7(c) demonstrates a significantly lower THD of 2.14%. This 1.53% reduction in THD confirms the proposed method's superior harmonic performance, particularly beneficial for Vienna rectifiers requiring enhanced input current quality.

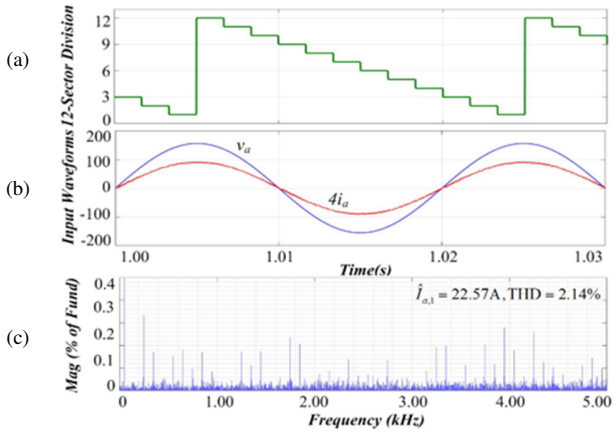

Fig. 7. Steady state results of the proposed rectifier operating under the proposed 12-sector SVPWM with PFC controller: (a) the 12-sector signal, (b) a-phase voltage and current waveforms, (c) a-phase current THD.

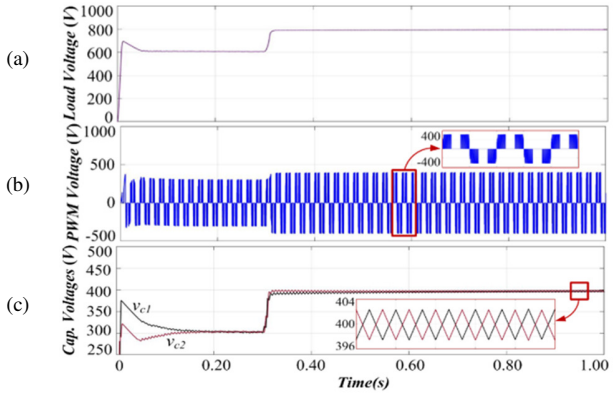

Fig. 8. Dynamic response of the proposed rectifier under DC-link voltage step changes: (a) DC-link voltage waveform, (b) the pole-to-neutral voltage waveform, and (c) the voltage across the two output capacitors.

Figure 8 illustrates the dynamic performance of the proposed Vienna rectifier in response to DC-link voltage steps. In Figure 8(a), the output voltage rises from 0V to 600V at

startup and then to 800V at 0.30s, with a transient settling time of approximately 12–15 ms, negligible overshoot, and minimal oscillation, confirming fast DC-link regulation. The pole-to-neutral PWM voltage (v_{AO}) in Figure 8(b) exhibits a three-level waveform of $+V_{dc}/2$, 0, and $-V_{dc}/2$. A clear DPWM clamping interval occurs at 0 V because the CPSs remain ON for about 3.33 ms in each half-cycle (≈6.66 ms/cycle), corresponding to one-third of the cycle. This significantly reduces switching commutations and improves thermal distribution. Figure 8(c) shows that the capacitor voltages v_{C1} and v_{C2} settle to approximately $V_{dc}/2$ within a few ms after each DC-link voltage step and maintain excellent voltage balance. The voltage ripples of both capacitors alternate within ±2.5V of $V_{dc}/2$ throughout operation without requiring any auxiliary balancing circuitry. Their rapid convergence with minimal deviation validates the correctness of the modified switching states and the proposed modulation signals, which remain fully consistent with the Vienna rectifier's inherent operating constraints. Furthermore, the results confirm that the proposed modulation strategy effectively coordinates with the widely used vector-based current control method, enabling a robust transient response as evidenced by the fast settling time and the absence of overshoot or oscillatory behavior following abrupt voltage changes. Such performance makes the approach well-suited for high-power industrial drives and DC fast-charging applications, where fast transient response and precise voltage regulation are essential.

VI. CONCLUSION

This study proposed a modified discontinuous modulation strategy for the Vienna rectifier, incorporating a novel 12-sector Space Vector Pulse Width Modulation (SVPWM), a topology-aware switching scheme, and a sector-based modulation offset-injection method. The proposed methodology enabled the systematic generation of modulation waveforms across all 12 sectors, thereby improving control of conduction intervals and alignment with the rectifier's operating constraints. Simulation results obtained in MATLAB/Simulink, both with and without Power Factor Correction (PFC), validated the effectiveness of the approach. In the low-modulation region (m_a<0.50), the proposed method achieved a 9.24% reduction in the Total Harmonic Distortion (THD) of the input current compared to the conventional 6-sector SVPWM. The PFC control further reduced the input current THD, from 3.67% to 2.14%. Additionally, the dynamic tests demonstrated rapid DC-link voltage recovery, reduced switching commutations (one-third/cycle), and stable capacitor-voltage balancing even under abrupt load variations. The proposed 12-sector SVPWM technique improves current quality, lowers switching losses, and dynamically controls voltage. This makes it a suitable choice for high-performance AC–DC conversion in applications like fast EV charging systems and industrial motor drives. Future research may focus on expanding the proposed strategy to address grid imbalances and common-mode voltage reduction, incorporating predictive or adaptive control, and validating the technique on hardware prototypes to assess real-time implementation challenges.

ACKNOWLEDGMENT

The authors would like to express their sincere gratitude to the faculty of industrial technology and the research and development Institute of Valaya Alongkorn Rajabhat University under the Royal Patronage for their continuous support and research funding that made this work possible.

REFERENCES

[1] P. Zhang *et al.*, "Reduction of Common-Mode Voltage and NP Voltage Oscillation for Three-Level Vienna Rectifiers Using Alternative Phase Opposition Disposition PWM," *IEEE Transactions on Industrial Electronics*, vol. 71, no. 8, pp. 8237–8247, Dec. 2024, https://doi.org/10.1109/TIE.2023.3317836.

[2] M. Bajaj, "A Brief Review of Power Quality Issues Emerged due to Modernization of Power System Infrastructure," *International Transactions on Electrical Engineering and Computer Science*, vol. 1, no. 1, pp. 8–25, Sept. 2022, https://doi.org/10.62760/iteecs.1.1.2022.5.

[3] I. Aretxabaleta, I. M. De Alegría, J. Andreu, I. Kortabarria, and E. Robles, "High-Voltage Stations for Electric Vehicle Fast-Charging: Trends, Standards, Charging Modes and Comparison of Unity Power-Factor Rectifiers," *IEEE Access*, vol. 9, pp. 102177–102194, Jun. 2021, https://doi.org/10.1109/ACCESS.2021.3093696.

[4] K. Hemasri and C. S. Kumar, "Fuzzy Controller with Shunt Active Power Filter in Reducing THD for Three Phase System," *International Transactions on Electrical Engineering and Computer Science*, vol. 3, no. 2, pp. 101–108, Jun. 2024, https://doi.org/10.62760/iteecs.3.2.2024.93.

[5] B. B, S. P, E. Pv, and M. Asif, "Energy-efficient Vienna rectifier for electric vehicle battery charging stations," *Results in Engineering*, vol. 23, Sept. 2024, Art. no. 102671, https://doi.org/10.1016/j.rineng.2024.102671.

[6] X. Feng, Y. Sun, X. Cui, W. Ma, and Y. Wang, "A compound control strategy of three-phase Vienna rectifier under unbalanced grid voltage," *IET Power Electronics*, vol. 14, no. 16, pp. 2574–2584, Oct. 2021, https://doi.org/10.1049/pel2.12202.

[7] Lan C., Huihui X., Qiang G. U. O., and Wenkai X., "Modified Carrier-based Pulse Width Modulation Strategy for Three-phase Vienna Rectifier," *Journal of Electrical Engineering*, vol. 16, no. 4, pp. 143–150, Dec. 2021, https://doi.org/10.11985/2021.04.018.

[8] Y. Zou, L. Zhang, Y. Xing, Z. Zhang, H. Zhao, and Z. Zheng, "A Unified Carrier-Based Pulsewidth Modulation for Three-Phase Vienna-Type Rectifiers," *IEEE Transactions on Power Electronics*, vol. 37, no. 5, pp. 5749–5762, Feb. 2022, https://doi.org/10.1109/TPEL.2021.3130065.

[9] Z. Shi, N. Li, Y. Yang, and Z. Fan, "A Novel Strategy for Current Distortion Suppression Based on Space Vector Modulation for Vienna Rectifiers Under the Wide-Range Unbalanced Grids," *IEEE Transactions on Power Electronics*, vol. 41, no. 2, pp. 2134–2147, Feb. 2026, https://doi.org/10.1109/TPEL.2025.3616142.

[10] W. Zhu, C. Chen, and S. Duan, "Model predictive control with improved discrete space vector modulation for three-level Vienna rectifier," *IET Power Electronics*, vol. 12, no. 8, pp. 1998–2004, Jun. 2019, https://doi.org/10.1049/iet-pel.2019.0040.

[11] O. Tubburee, C. Photong, N. Angkawisittpan, K. Ek-iam, and W. Sangiamvibool, "Design and Development of Three-Phase Two-Level Unidirectional Rectifiers for EV Chargers Using SVPWM and a Voltage-Oriented Controller," *Engineering, Technology & Applied Science Research*, vol. 15, no. 5, pp. 27877–27884, Oct. 2025, https://doi.org/10.48084/etasr.12947.

[12] H. Ma, Y. Lu, K. Zheng, and T. Xu, "Research on the Simplified SVPWM for Three-Phase/Switches Y-Type Two-Level Rectifier," *IEEE Access*, vol. 8, pp. 214310–214321, Nov. 2020, https://doi.org/10.1109/ACCESS.2020.3041283.

[13] Y. Zou *et al.*, "Dynamic-Space-Vector Discontinuous PWM for Three-Phase Vienna Rectifiers With Unbalanced Neutral-Point Voltage," *IEEE Transactions on Power Electronics*, vol. 36, no. 8, pp. 9015–9026, Dec. 2021, https://doi.org/10.1109/TPEL.2021.3057120.

[14] Y. Zou, L. Zhang, Y. Xing, K. Sun, C. Huang, and Z. Li, "A Modified Carrier-Based PWM with High DC Voltage Utilization for Three-Level Inverters with Unbalanced Neutral-Point Voltage, " in *2025 IEEE Energy Conversion Congress & Exposition Asia (ECCE-Asia)*, Feb. 2025, pp. 1–5, https://doi.org/10.1109/ECCE-Asia63110.2025.11112420.

[15] W. Zhu, C. Chen, S. Duan, T. Wang, and P. Liu, "A Carrier-Based Discontinuous PWM Method With Varying Clamped Area for Vienna Rectifier," *IEEE Transactions on Industrial Electronics*, vol. 66, no. 9, pp. 7177–7188, Sept. 2019, https://doi.org/10.1109/TIE.2018.2873524.

[16] T.-L. Le, "A Robust Control Strategy for Effective Field-Oriented Control of PMSMs," *Engineering, Technology & Applied Science Research*, vol. 14, no. 6, pp. 18469–18475, Dec. 2024, https://doi.org/10.48084/etasr.8893.